Eur. Phys. J. Appl. Phys. **89**, 30801 (2020)

https://doi.org/10.1051/epjap/2020200011

THE EUROPEAN PHYSICAL JOURNAL APPLIED PHYSICS

Regular Article

A study of line-plane configuration in the Corona discharge theory

Asep Yoyo Wardaya[1,2,*], Zaenul Muhlisin[1,3], Alam Hudi[1], Jatmiko Endro Suseno[1], Muhammad Nur[1,3], Andi Wibowo Kinandana[1,3], and Jaka Windarta[2]

[1] Department of Physics, Faculty of Science and Mathematics, Diponegoro University, Semarang, Indonesia
[2] Master of Energy Program, School of Post Graduate Studies, Diponegoro University, Semarang, Indonesia
[3] Center for Plasma Research, Diponegoro University, Semarang, Indonesia

Received: 17 January 2020 / Received in final form: 24 February 2020 / Accepted: 12 March 2020

Abstract. Research on corona discharges from plasma generators has been studied using the line-plane configurations (L-PC). The purpose of this study is to calculate the comparison of the level of conformity of the voltage current characteristic curve (I–V) from the simulation results of numerical calculations of the electrode geometry function and the results of experimental data. There is an electrode (electrode 1) in the form of a rectangular plate with a very thin thickness which has a length and width of a and b respectively in an upright position (line configuration). Electrode 1 has a distance of c to electrode 2 which is in a lying position (plane configuration) below the electrode 1. Furthermore, by using variation of c of 2.5 cm, 2.8 cm, 3.1 cm and 3.4 cm, the two electrodes are connected to the plasma generating equipment, thus producing a plasma discharge that comes out of the tip of the electrode 1 towards electrode 2. Research results from all variations of c prove that there is a high degree of suitability between numerical calculations with experimental data by taking the value of the fitting for the sharpness shape factor of k in the area with the largest plasma discharge.

1 Introduction

Plasma is gas which is ionized in an electric discharge [1]. When gas is conditioned on a plasma state, charged particles in the gas have a smaller potential energy among inter particles compared to their kinetic energy so that the particles are free to move [2]. Plasma generation through the concept of electrical discharge is known as corona incandescent plasma discharge [3,4]. There is a common plasma model in the industry called capacitively coupled plasma (CCP) [5,6]. The electrode configuration of the CCP is similar to the principle of a capacitor in an electronic circuit. This model consists of two asymmetrical electrodes with one electrode having a very sharp surface and the other electrode having a nearly horizontal surface. Incandescent corona plasma discharges will appear around the electrode with high/sharp curvature due to the area having a high gradient potential [7]. This fact that supports the dependence of the electric current value on the electrode geometrical curvature in the case of the corona discharge is that the geometrical shape of the electrode which is sharper will produce a plasma flow that is getting bigger.

Numerous papers on corona discharge cases or ordinary electrical circuits using capacitor or CCP components often discuss the characteristics curves of current and voltage from all sorts of electrode configurations. These configuration models include tip-plane configuration [8], cylinder-wire-plate configuration [9], sub-millimeter electrode gap configuration [10], point-to-ring configuration [11], needle-to-plate configuration [12], multi point-plane configuration [13] and coaxial Cylinders [14]. Most discussions concerning characteristic models of current and voltage system are only experimental, except for journals of [8,14], which detailed the (I–V) characteristic curves from numerical calculations as well as comparisons with experimental results. There is a very striking difference in the (I–V) characteristic value ratio between [8] and [14]. The (I–V) characteristic of [8] is based on the geometrical shape of the electrode capacitance in the case of an ordinary electric circuit while the (I–V) characteristic of [14] uses the corona discharge curve approach formula. The value of the electric current obtained from [14] is almost close to 10^6 times the value of the electric current from [8].

There are also several papers that discuss the concept of corona discharge not focused on the formulation of (I–V) characteristic curves and the configuration of the electrodes (curvature of the electrodes geometry) but instead discusses the influence of certain factors when event happened of corona discharges such as EHD flow [11], convective heat transfer [15], electric wind [16,17] and electrostatic precipitation [18,19]. From papers [15–19], it can be concluded that corona discharge is a fairly complex physical event, so that the (I–V) characteristic curves are not only influenced by the curvature of the electrodes geometric but also influenced by other factors such as convective heat transfer, electric wind and electrostatic

* e-mail: asepyoyowardayafisika@gmail.com

precipitation. Of course, if all of the above factors are taken into account in the case of the calculation of the (I–V) characteristic curves for the line-plane configuration (L-PC) model in this paper, it will produce a very complex equation to be discussed.

The line-plane configuration (L-PC) model of corona plasma discharge case consists of electrodes in the shape of two thin and sharp capacitor plates positioned perpendicular, with the first electrode stands straight up on top of the laid second electrode in the horizontal position (CCP models). When current flows between the two electrodes, the result is the corona plasma discharge that yields electric plasma current. This research comes with a novelty of complete discussion as it takes both numeric and experimental results into account by comparing characteristics curves from experimental data with that of numerical calculation. The focus of research on the L-PC model is the capacitance calculation on the sharp geometric surface of the capacitor in an upright position will produce a very large electric plasma flow compared to other surfaces. In the capacitance calculation is adding a sharpness shape factor k (with a large value) to the capacitor with sharp geometry to meet the very large electric current value requirements of the plasma cases. The factor k value is determined from the fitting ratio between the results of numerical and experimental calculations.

2 Experimental results

The research scheme for electrode 1 used a very thin rectangular plate (0.1 mm thickness) of length a and width b positioned perpendicular against the electrode 2 lay down, with the perpendicular distance between the first and the second electrodes denoted as c. Both electrodes were then connected to voltage V so that the first electrode generates plasma flow that will be collected by the second electrode. The research scheme is shown in Figure 1.

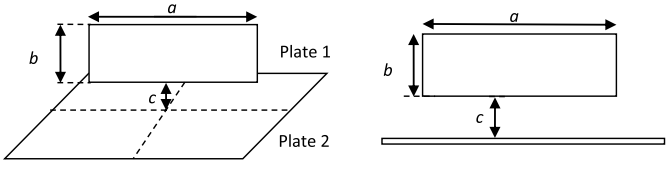

(*a*) (*b*)

Fig. 1. (a) Scheme of the L-PC electrode model. (b) The L-PC model is viewed from the side.

The equipment scheme used in this study is shown in Figure 2. The equipment is used consisted of a rectangular metal for electrode 1 (anode) with thin thicknesses having length $a = 7.75$ cm, width/height $b = 1.4$ cm, and thickness $\delta = 0.1$ mm. The second electrode (cathode) are used in metal-shaped metal containers filled with the palm oil as high as 1 mm from the bottom surface. The position of electrode 1 is perpendicular to the electrode 2. The function of palm oil at the electrode 2 is to see the effect of plasma flow is caused by the corona discharge process.

Electrodes with line-plane configuration are connected to DC high voltage generators with a voltage of 4 kV and a frequency of 25 kHz. Electric current is measured using an analog Multimeter have branded SANWA by type YX-360TREB, voltage 220 V, frequency 50/60 Hz arranged in series from the circuit. Measurement of potential differences is done by using digital multimeter have branded SANWA by type CD771. The electric current used to measure variations of potential differences in the multimeter (Voltmeter) is passed first through the HV probe (DC max Voltage DC 40 kV, AC 28 kV model number PD-28, Serial number 01605733), with the HV probe function is to convert the value of kV becomes Volt.

Experiment results show that electric fields flow from along thin surface lines and both the lower edges of the first electrode heading for the second electrode, with the largest electric field emerging from the both the lower edges, which can be detected by the appearance of changes in the waveform of the oil on the second electrode as shown in Figure 3.

The magnitude of electric field stemming from the lower side of the first rectangular electrode in Figure 3 (the L-PC electrode model) is of two parts:

1. The electric field that arises from the path of the bottom straight line area in the electrode 1.

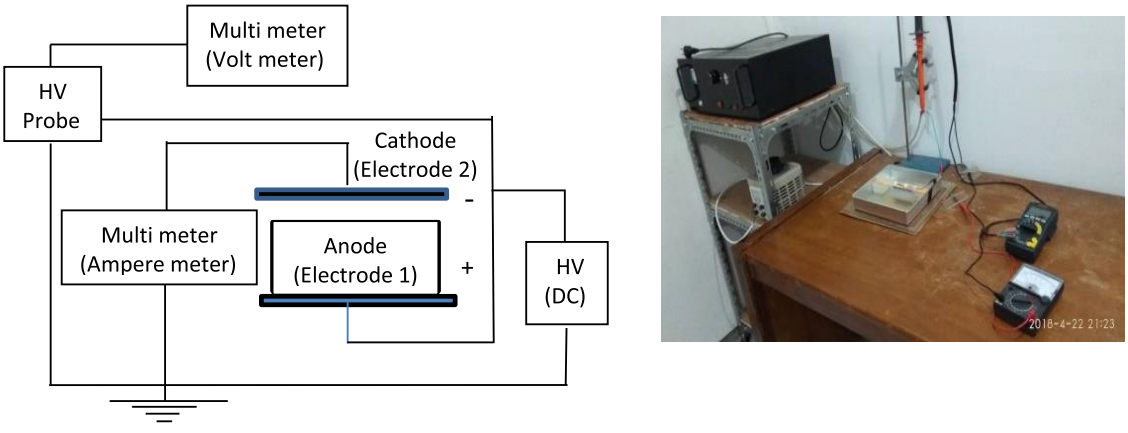

(*a*) (*b*)

Fig. 2. (a) Research equipment scheme for the corona discharge. (b) Photo of Research equipment.

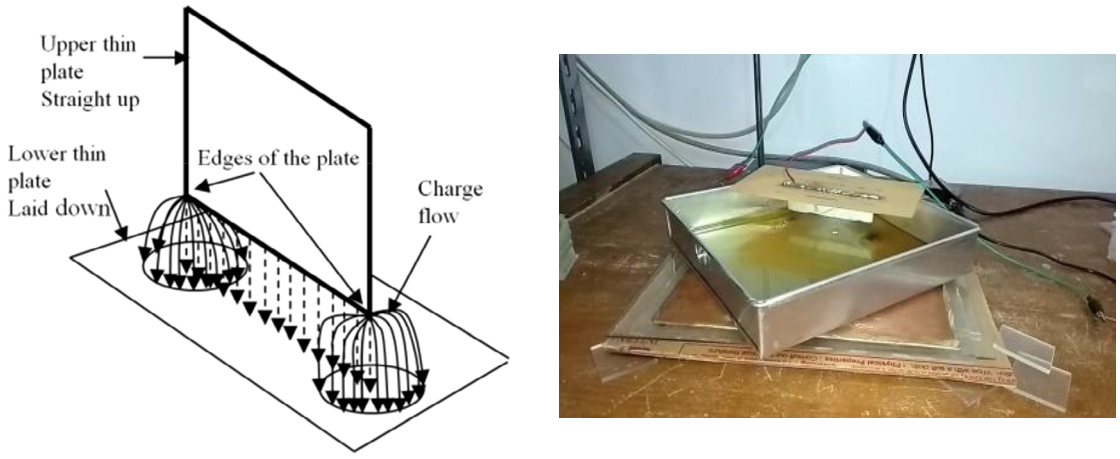

Fig. 3. (a) Scheme of plasma electric charges flow coming out of the L-PC electrode model. (b) Photo of research results, with the oil liquid was added to see the effect of plasma discharge on the surface under electrode 1.

2. The electric field from the left and right edges of the lower electrode area has the greatest value.

3 Mathematical models

Before discussing the numerical calculations of the L-PC electrode model, we will discuss a formulaic approach [8] from the electric current I to voltage V for the case of the ordinary electric circuit as,

$$I = \frac{\pi}{0.78} \in \mu \frac{V^2}{c}, \tag{1}$$

where c is the distance between the two capacitive electrodes and the number 0.78 is an approach value of the formula, while the (I–V) characteristic curves [14] by Townsend's in the CCP case using the corona discharge curve approach formula in the currents low case is written as

$$I = 10^6 \frac{8\pi \in b_0}{\delta R^2 \ln(R/r)} V(V - V_0), \tag{2}$$

where V_0 is the initial voltage of the corona, δ is the critical density of gas (air), R (cm) and r (cm) respectively are the outer radius of the cylinder (outer electrode) and the radius of the wire (inner electrode) and b_0 is ion mobility [(m/s)/(V/m)] at $\delta = 1$. From the comparison of equations (1) and (2) it can be seen that the current value in the corona discharge event (Eq. (2)) is almost close to 10^6 of the ordinary electric circuit current in equation (1). Whereas corona discharge events covering Townsend's low current curves and followed by medium to high current curves (corona discharge curves) [14], which is of course the value of the electric current will be greater on the medium to high current curves compared to the low currents in equation (2). The very large current in the corona discharge case arises from the extremely sharp electrode geometrically surface of the CCP model [7].

Prior to discussing the calculation for the L-PC electrode model as shown in Figure 1, a model of two capacitor electrodes should be reviewed. The thin electrode 1 here is of $a.b$ area with inclination angle $\in \ll 1$ against the vertical plane. Meanwhile, the second electrode is laid a c distance away from the first electrode, as shown in Figure 4.

Let's say that between the two electrodes is voltage V. In order to calculate the capacitance of that capacitor system, area of the first electrode is divided into elements of length a and width dx or the element area is $a\ dx$, that projection of that element on the second electrode is equal to $a\ dx$. Distance of x on the second electrode as shown in Figure 4a is within range,

$$0 \le x \le b \sin \in, \tag{3}$$

where the definition of element area dA and distance h between area of electrode 1 and that of electrode 2 is

$$dA = a \cdot dx \ \text{ and } \ h = x cot \in + c. \tag{4}$$

The magnitude of capacitance of both electrode area elements can be written as

$$dC = \varepsilon_0 \frac{dA}{h} = \frac{\varepsilon_0 a dx}{(x cot \in + c)}, \tag{5}$$

with the total capacitance of both electrodes shown in Figure 4b is

$$C = \varepsilon_0 a \int_{x=0}^{b\sin\in} \frac{\mathrm{d}x}{(x cot \in + c)} = \varepsilon_0 a \ln \left| \frac{b\cos \in + c}{c} \right|. \tag{6}$$

For the L-PC electrode model (Fig. 4b), the first electrode is positioned perpendicular to the second electrode, or $\in \cong 0$, that the capacitance of the first

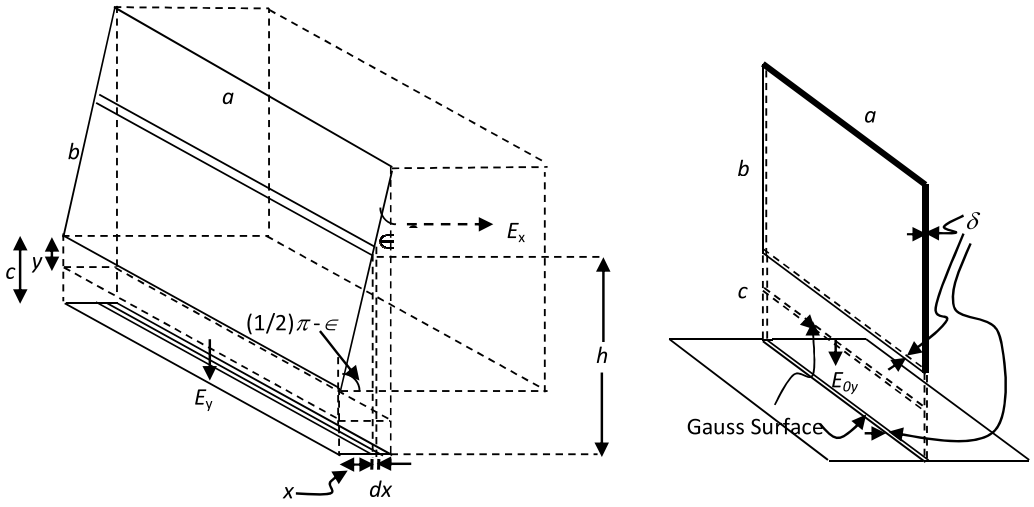

Fig. 4. (a) Scheme of electrode model with the first electrode is positioned almost perpendicular to the second electrode. (b) The depiction of the electric field E_{0y} in the case of two electrodes in a perpendicular position each other.

electrode is perpendicular to the second electrode as follow

$$C_{0y} = \varepsilon_0 a \ln\left|\frac{b}{c} + 1\right|. \tag{7}$$

The magnitude of the electric field perpendicular to plate 2 in the L-PC case (in the y-axis direction) can be calculated from equation (7) using the Gauss formula,

$$\varepsilon_0 \oint \mathbf{E}_y . d\mathbf{A} = \varepsilon_0 E_{0y} a\delta = q_{0y}, \quad \delta \cong 0.1\,\text{mm}. \tag{8}$$

Using the definition of charge $q_{0y} = \Delta V . C_{0y}$, where ΔV is voltage between the electrodes. Hence, the magnitude of electric field in y-axis for L-PC electrode model is,

$$E_{0y} = \frac{\Delta V}{\delta} \ln\left|\frac{b}{c} + 1\right|, \tag{9}$$

where the magnitude of electric field in x-axis is zero, as all electric fields are in the y-axis direction.

The experiment here took the case of $b < c$. The scheme for electric field flow E_{0y} is shown in Figure 4b. In fact, if you look at the results of the experiment in Figure 3, the largest plasma flow (showing the flow of electric charge) actually appears from the two sharp ends at the bottom of the electrode 1 which is detected by the movement of larger oil waves below the sharp edges of the electrode 1 compared to below the surface of the straight line from the electrode 1. This fact shows that the geometrical shape of the electrode which is getting sharper will produce a greater plasma flow as well. In this study, the angle of plasma flow out from the two ends of the plate is on average around 60° to the vertical plane, as shown in Figure 5a.

To calculate the magnitude of the electric field coming out from both sharp edges at points A and B of the electrode 1 in Figure 5a, using the electrode geometry approach and using the concept of Gauss's law, then the first thing to do is calculate the capacitance model in the case of Figure 5a (only at point A) by referring to equation (7) for the capacitance model in Figure 4b. Because the plasma current flowing out of the edges of the rectangular plate forms an angle of 60° with a vertical plane so that the length of the plasma flow path from electrode 1 to electrode 2 is equal to $l = 2c$. For reference capacitance calculation in Figure 4b., requires that the plasma flow path is straight from electrode 1 to electrode 2, so that the capacitance calculation in Figure 5a is made the approach of the plasma current flow path A0 is straight from the ABGF plate to the plate below it as far as $l = 2c$. This makes the position of the ABGF plate sharpen, as shown in Figure 5b, with the 0AF axis being the vertical axis h and the flat axis is the u-axis and the sharp point of the ABGF plate is point A. To calculate the capacitance approach of the ABGC sharped plate to the plate which is considered to be located at point 0, the plates are divided into triangular plates so that the total capacitance on the sharped part is

$$C_{\text{pointed}} = \lim_{k \longrightarrow \text{big value}} k(C_{ABE} + C_{ACD}) + C_{CDF} + C_{EBH} - C_{FGI} - C_{IGH}. \tag{10}$$

The addition of the sharpness shape factor of k (with a very large value) to the ABE and ACD triangles capacitance, due to the lower end of the two triangles is located right at point A which is the pointed end of the ABGC plate. In Figure 3 it has been shown that at both ends of the sharp plate will produce a very large plasma flow compared to the other plates.

As one example of the calculation of the triangular plates in equation (10), the capacitance value of the ABE triangle plate will be calculated against the plate which is considered to be located at point *0*. Using the comparison

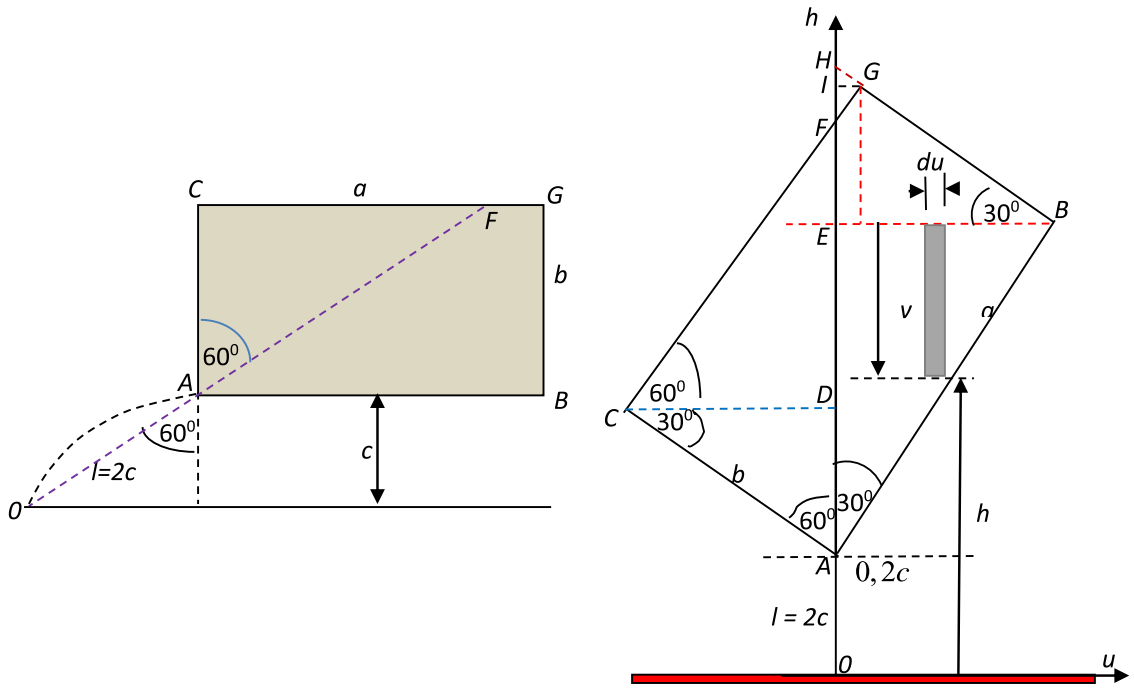

(*a*) (*b*)

Fig. 5. (a) The model of plasma flow that coming out from one side of electrode sharp surface. (b). Capacitance calculation model of the plasma flow at figure *a*.

of equation (7) for the plate case in Figure 4b, the magnitude of the capacitance element of the ABE triangle plate is

$$dC_{ABE} = \varepsilon_0\, du \ln\left|\frac{v}{h}+1\right|, \quad \text{with}$$
$$0 < u < \tfrac{1}{2}a. \tag{11}$$

There is a constant value of the sum of $v+h$ which is the path length from point 0 to point E, where the value of the variable h as a function u is defined as,

$$v + h = l_{0E} = \tfrac{1}{2}a\sqrt{3} + 2c, \quad \text{with}$$
$$h = u\sqrt{3} + 2c. \tag{12}$$

By using equations (11) and (12), the capacitance value of the triangle ABE can be written as

$$C_{ABE} = \varepsilon_0 \int_{u=0}^{\frac{1}{2}a} ud \ln\left|u\sqrt{3}+2c\right|$$
$$= \varepsilon_0 \left\{\frac{1}{2}a - \frac{2c}{\sqrt{3}} \ln\left|\frac{\frac{1}{2}a\sqrt{3}+2c}{2c}\right|\right\}. \tag{13}$$

For other triangular capacitance calculations, you can see in Table 1.

By using equations (10) and Table 1, we get the amount of capacitance pieces from the sharped portion on the lower left side of the triangle ABGC as,

See equation (14) below

$$C_{pointed} = \lim_{k \longrightarrow big\ value} k \left\{ \varepsilon_0 \frac{1}{2}\, a + \frac{1}{2} b\varepsilon_0\sqrt{3} - \varepsilon_0 \frac{2c}{\sqrt{3}} \ln\left|\frac{\frac{1}{2}a\sqrt{3}+2c}{2c}\right| - 2c\varepsilon_0\sqrt{3} \ln\left|\frac{\frac{3}{2}b+6c}{6c}\right| \right\}$$
$$+ \frac{3}{2}\,\varepsilon_0 b\sqrt{3} + \varepsilon_0 \left[\frac{1}{2}b\sqrt{3} - \frac{2(b+c)}{\sqrt{3}}\right] \ln\left|\frac{2(b+c)}{\frac{1}{2}b+2c}\right| - \frac{1}{2}a\varepsilon_0 - \varepsilon_0\left(2c\sqrt{3}+\frac{3}{2}a\right) \ln\left|\frac{\frac{2}{3}a\sqrt{3}+2c}{2c+\frac{1}{2}a\sqrt{3}}\right|$$
$$+ \frac{\varepsilon_0(2b+2c)}{\sqrt{3}} \ln\left|\frac{\frac{1}{2}\,a\sqrt{3}+\frac{1}{2}b+2c}{2b+2c}\right| - \varepsilon_0\left(\frac{1}{2}\,b\sqrt{3}+2c\sqrt{3}+\frac{3}{2}a\right) \ln\left|\frac{\frac{1}{2}\,b+2c+\frac{1}{2}a\sqrt{3}}{2c+\frac{2}{3}a\sqrt{3}}\right|. \tag{14}$$

Table 1. The fractional triangle capacitance values of the $ABGC$ plate capacitance values at the pointed end at point A.

No△	Integration limits	$v+h$	$h=f(u)$	Capacitance C
1. ABE	$0<u<\frac{1}{2}a$	$\frac{1}{2}a\sqrt{3}+2c$	$u\sqrt{3}+2c$	$\varepsilon_0\left\{\frac{1}{2}a-\frac{2c}{\sqrt{3}}\ln\left\lvert\frac{\frac{1}{2}a\sqrt{3}+2c}{2c}\right\rvert\right\}$
2. ACD	$-\frac{1}{2}b\sqrt{3}<u<0$	$\frac{1}{2}b+2c$	$-\frac{1}{3}u\sqrt{3}+2c$	$\varepsilon_0\left\{\frac{1}{2}b\sqrt{3}-2c\sqrt{3}\ln\left\lvert\frac{\frac{3}{2}b+6c}{6c}\right\rvert\right\}$
3. CDF	$-\frac{1}{2}b\sqrt{3}<u<0$	$2b+2c$	$u\sqrt{3}+2b+2c$	$\frac{1}{2}\varepsilon_0 b\sqrt{3}+\varepsilon_0\left\{\frac{1}{2}b\sqrt{3}-\frac{2(b+c)}{\sqrt{3}}\right\}\ln\left\lvert\frac{2(b+c)}{\frac{1}{2}b+2c}\right\rvert$
4. EBH	$0<u<\frac{1}{2}a$	$\frac{2}{3}a\sqrt{3}+2c$	$-\frac{1}{3}u\sqrt{3}+2c+\frac{2}{3}a\sqrt{3}$	$\frac{1}{2}a\varepsilon_0-\varepsilon_0\left(2c\sqrt{3}+\frac{3}{2}a\right)\ln\left\lvert\frac{\frac{2}{3}a\sqrt{3}+2c}{\frac{1}{2}a\sqrt{3}+2c}\right\rvert$
5. FGI	$0<u<\frac{1}{2}a-\frac{1}{2}b\sqrt{3}$	$2c+\frac{1}{2}a\sqrt{3}+\frac{1}{2}b$	$u\sqrt{3}+2b+2c$	$\frac{1}{2}\varepsilon_0 a-\frac{1}{2}\varepsilon_0 b\sqrt{3}-\frac{\varepsilon_0(2b+2c)}{\sqrt{3}}\ln\left\lvert\frac{\frac{1}{2}a\sqrt{3}+\frac{1}{2}b+2c}{2b+2c}\right\rvert$
6. IGH	$0<u<\frac{1}{2}a-\frac{1}{2}b\sqrt{3}$	$2c+\frac{2}{3}a\sqrt{3}$	$-\frac{1}{3}u\sqrt{3}+2c+\frac{2}{3}a\sqrt{3}$	$\frac{1}{2}\varepsilon_0 a-\frac{1}{2}\varepsilon_0 b\sqrt{3}+\varepsilon_0\left(\frac{1}{2}b\sqrt{3}+2c\sqrt{3}+\frac{3}{2}a\right)\ln\left\lvert\frac{\frac{1}{2}b+2c+\frac{1}{2}a\sqrt{3}}{2c+\frac{2}{3}a\sqrt{3}}\right\rvert$

The Gauss surface with the value of $\delta\cong 0.1$ mm is defined as $A=\delta(b\sin 60^\circ+a\sin 30^\circ)+\delta^2=\delta(\frac{1}{2}\,b\sqrt{3}+\frac{1}{2}\,a)+\delta^2$. By using Gauss's law, the value of the electric field is obtained on the sharp plate as,

$$E_{\text{pointed}}=\frac{q}{\varepsilon_0 A}=\frac{\Delta V C_{\text{pointed}}}{\varepsilon_0\left\{\delta\left(\frac{1}{2}\,b\sqrt{3}+\frac{1}{2}a\right)+\delta^2\right\}}. \tag{15}$$

The total current that occurs comes from electric currents from the thin plate as well as two sharp plate parts (bottom left and right end of the plate) by definition $q_{\text{pointed}}=\Delta V\ C_{\text{pointed}}$, $\Delta V=V-V_i$, where V is the voltage used and V_i is the voltage of the corona threshold. The total electric current generated by the L-PC electrode model of length a, width b and thickness δ, where $q_{0y}=\Delta V\ C_{0y}$, is [8],

See equation (16) below

with the C_{pointed} value indicated by the equation (14). If you see the arrangement of the electrodes in Figure 3b is the same as the series arrangement of 2 capacitors consisting of capacitors without dielectric (filled with air) C_0 and with dielectric (containing oil) C_k, which can be written as

$$C_0=\varepsilon_0\frac{A}{d_1},\quad\text{and}\quad C_k=k_p\varepsilon_0\frac{A}{d_2},\quad d_2\ll d_1, \tag{17}$$

where d_1 is the distance from the tip of the electrode 1 to the oil surface and d_2 is the oil surface height to the electrode 2 (1 mm). For a series arrangement, the total capacitor value can be written as

$$C_{\text{tot}}=\frac{C_0}{1+\left({}^{C_0}/_{C_k}\right)}=\frac{C_0}{1+\left({}^{d_2}/_{d_1 k_p}\right)}\cong C_0, \tag{18}$$

$$\begin{aligned} i=\frac{dQ}{\mathrm{d}t}&=\frac{\mu_0}{\Delta V}\left(qE^2\right)_{total}=\frac{\mu_0}{\Delta V}\left\{q_0 {E_{0y}}^2+2|q_{\text{pointed}}||E_{\text{pointed}}|^2\right\}\\ &=\mu_0\varepsilon_0\left\{\frac{a}{\delta^2}(V-V_i)^2(\ln|(b/c)+1|)^3+\frac{2(V-V_i)^2\left(C_{\text{pointed}}\right)^3}{{\varepsilon_0}^3\left\{\delta\left(\frac{1}{2}\,b\sqrt{3}+\frac{1}{2}\,a\right)+\delta^2\right\}^2}\right\} \end{aligned} \tag{16}$$

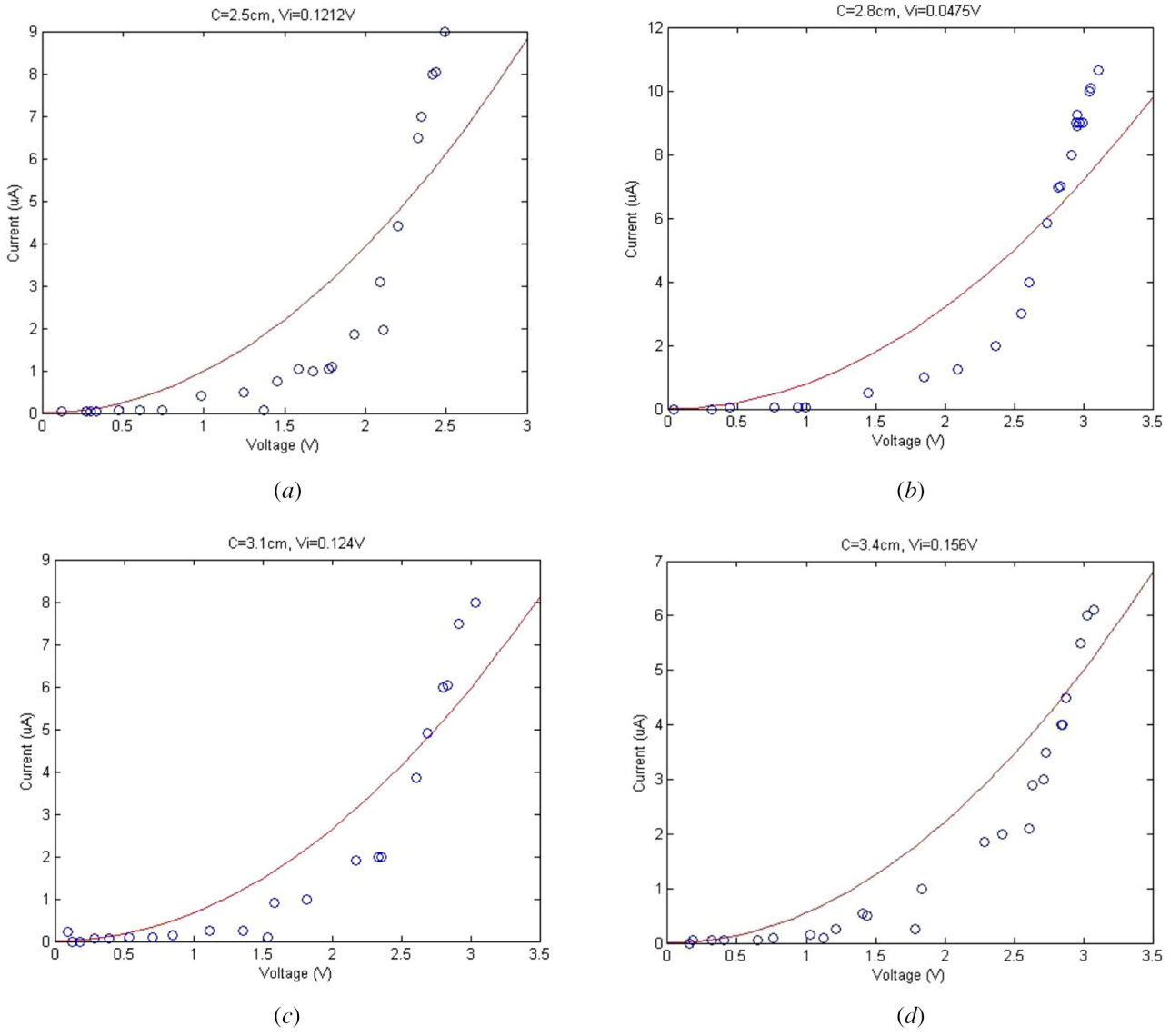

Fig. 6. The (I–V) characteristics curves from the corona plasma discharge with the L-PC electrode model of c values variation for (a) 2.5 cm, (b) 2.8 cm, (c) 3.1 cm and (d) 3.4 cm, with the fitting ratio of the sharpness shape factor of k is 7000.

where the values of $d_2 = 1$ mm, $d_1 = 24$ mm (lowest value) and the dielectric constant for palm oil have been taken $k_p = 3.1$ [20].

Equation (16) formulates the current versus voltage function of the corona plasma charge generated by the L-PC electrode model using very thin electrodes positioned perpendicular to one another.

4 Results of simulation and experiment

The research here employed straight up rectangular electrode (the first electrode) of length $a = 7.75$ cm, width/height $b = 1.4$ cm, and thickness $\delta = 0.1$ mm, while the areas of the laid down electrode (the second electrode) is enough to collect all plasma flow from the first electrode. Distances between the two electrodes edges c are varied, as shown in Figure 6; (a) with $c = 2.5$ cm and $V_i = 0.1212$ Volt, (b) with $c = 2.8$ cm and $V_i = 0.0475$ Volt and (c) with $c = 3.1$ cm and $V_i = 0.124$ Volt and (d) with $c = 3.4$ cm and $V_i = 0.156$ Volt.

Using equation (16) for varied c of 2.5 cm, 2.8 cm, 3.1 cm and 3.4 cm, results in simulation graphs for various electric current I and voltage V or (I–V) characteristics curves. These simulation graphs will then be compared with experiment graphs of the same variations of electric current I and voltage V, with the fitting ratio of the multiplier factor value of k is 7000 (Fig. 6).

5 Discussion

In this chapter, we will discuss the level of concordance between simulations of mathematical numerical calculations with experimental data from the function of the characteristics of electric current vs voltage using the L-PC

electrode model. From the characteristic curves in Figure 6a–d, based on the author's observations there is a fairly high level of suitability between the simulation results and research data by taking a fitting of 7000 for the factor value of k. From the results of comparing experimental results with numerical calculation results, it can be concluded that

- There is a high level of suitability between the experimental data and the line equation from the results of numerical calculations on the fitting value of the factor $k = 7000$.
- The fitting value of a factor k that is large enough indicates that the value of the electric current generated by the plasma discharge is far greater than that of an ordinary electric circuit. The difference in current value is due to the plasma discharge reaction being influenced by various physical problems such as EHD flow [11], convective heat transfer [15], electric wind [16,17] and electrostatic precipitation [18,19], etc.

Some possibilities deviations of experimental data with the results of numerical calculations can be caused by the following factors are

- The accuracy less level of observations and measuring plasma reactor equipment.
- The level of precision is less smooth at along the sharpness line of the electrode 1.
- There is an energy loss factor from the plasma reactor equipment.

6 Conclusions

The electric current numeric calculation model as a potential function using the geometrical concept of the capacitively electrodes has been obtained quite in match with the experimental results data on the (I–V) characteristic curves of the corona plasma discharge using a L-PC electrode model. In this case a new numerical research model is used, namely the calculation of capacitance by adding a multiplier factor value of k. The k factor is needed to connect the concept of an electric current generated by an ordinary electric circuit with a corona plasma discharge specifically through the calculation of capacitance on the sharp electrode surface. In the case of corona plasma discharges, a sharp surface shape will produce a very large flow of plasma electricity because in that area will have a high gradient potential.

This work was financially supported by non-tax revenue (PNBP), Diponegoro University, Semarang, Indonesia under contract No. 329-91/UN7.P4.3/PP/2019.

Author contribution statement

Asep Yoyo Wardaya: Mathematical model, numerical calculation and writing part manuscript. Zaenul Muhlisin: preparation of research equipment and experimental work. Alam Hudi: experimental work. Jatmiko Endro Suseno: Simulation Program, discussion and writing part manuscript. Muhammad Nur: discussion and writing part manuscript. Andi Wibowo Kinandana: discussion and experimental work. Jaka Windarta: preparation of research equipment and discussion.

References

1. J. Allen, Plasma Sources Sci. Technol. **18**, 1 (2008)
2. D.R. Nicholson, *Introduction to Plasma Theory* (John Wiley & Sons, New York, 1983)
3. B. Champman, *Glow Discharge Processes* (John Willey & Sons, New York, 1990)
4. J.S. Chang et al., IEEE Trans. Plasma Sci. **19**, 1152 (1991)
5. A. Boudghene, Stambouli, R. Benallal, N. Oudini, S. M. Mesli, R. Tadjine, Eur. Phys. J. Appl. Phys. **80**, 1 (2017)
6. P. Saikia, H. Bhuyan, M. Escalona, M. Favre, E. Wyndham, J. Maze, J. Schulze, Plasma Sources Sci. Technol. **27**, 1 (2018)
7. E.M. van Veldhuizen, W.R. Rutgers, Corona Discharges: Fundamental and Diagnostics, in *4th Frontiers in low temperature plasma diagnostics* (2001), pp. 40–49
8. R. Coelho, J. Debeau, J. Phys. D: Appl. Phys. **4**, 1266 (1971)
9. L.M. Dumitran, L. Dascalescu, P.V. Notinger, P. Atten, J. Electrostat. **65**, 758 (2007)
10. R. Tirumala, Y. Li, D.A. Pohlman, D.B. Go, J. Electrostat. **69**, 36 (2011)
11. V.T. Dau, T.X. Dinh, T. Terebessy, T.T. Bui, J. Electrostat. A **244**, 146 (2016)
12. S. Kanazawa, T. Ito, Y. Shuto, T. Ohkubo, Y. Nomoto, J. Mizeraczyk, J. Electrostat. **55**, 343 (2002)
13. Jaworek, A. Krupa, J. Electrostat. **38**, 187 (1996)
14. J.S. Townsend, Philos. Mag. (London) **28**, 83 (1914)
15. M. Robinson, Int. J. Heat Mass Transfer **13**, 263 (1970)
16. M. Robinson, Trans. Am. Inst. Electr. Eng. Part I **80**, 143 (1961)
17. M. Robinson, Am. J. Phys. **30**, 366 (1962)
18. M. Robinson, J. Air Pollut. Control Assoc. **18**, 235 (2012)
19. J.R. Bush, P.L. Feldman, M. Robinson, J. Air Pollut. Control Assoc. **29**, 365 (2012)
20. G. Elert, Dielectrics-The Physics Hypertextbook (1998–2019) https://physics.info/dielectrics/

Cite this article as: Asep Yoyo Wardaya, Zaenul Muhlisin, Alam Hudi, Jatmiko Endro Suseno, Muhammad Nur, Andi Wibowo Kinandana, Jaka Windarta, A study of line-plane configuration in the Corona discharge theory, Eur. Phys. J. Appl. Phys. **89**, 30801 (2020)